FEM SIMULATIONS OF TEMPERATURE DISTRIBUTION OF GAAS SINGLE CRYSTAL USING THE CZOCHRALSKI (CZ) GROWTH TECHNIQUE

OGBONDA, CLEMENT
Department of Physics
Ignatius Ajuru University of Education
Rumuolumeni, Port Harcourt. Rivers State Nigeria

And

WAGBARA, EVERREST WENENDA
Department of Physics,
Ignatius Ajuru University of Education,
Rumuolumeni. Port Harcourt. Rivers State Nigeria

Abstract

A theoretical model is presented which enables temperature distribution during Czochralski growth of Gallium Arsenide (GaAs) single crystal to be studied. It was observed that thermal stresses are induced by temperature variations in gallium arsenide (GaAs) crystal growth. The thermal stresses causes plastic deformations by cracks, dislocation, defect and dynamic interaction in the crystal. As the temperature increases, the pull rate increases , the radius of the crystal increases, the temperature distribution is more, also the most effective way to reduce solid-liquid interfacial temperature gradients is to increase the diameter of the crystal; this implies that it may be easier to grow large crystals with low temperature distribution and thermal stresses than small crystals.The temperature distribution in the Czochralski technique (CZ) growth of GaAs crystal obtained is in agreement with Jordan model.

Key words; Temperature distribution, Czchralski growth, single crystal, Gallium arsenide, pull rate, time.

Numeclatures

h	the local heat generation in unit volume
G	Gibbs free energy or Gebhart factor
f	View factor
T	the temperature,
k	the thermal conductivity
e_n	a normal of the surface
q	the heat flux
h_T	the heat transfer coefficient,
σ_{SB}	the Stefan-Bolzmann constan
f_{ij}	the view factor between two surface elements
U	test function space

T_{ext} the external temperature
G_{ji} the discrete Gebhart factor
i_s the number of surface elements
ϵ the emissivity of the surface,
T_{ext} some external temperature
$G.(r^{\rightarrow 1}, r^{\rightarrow})$. the *Gebhart factor*
A_i the area of an surface element i
i the number of nodes.
φ_i basis functions
t_i unknown temperatures at selected points

Introduction

Czochralski technique (CZ) (Czochralski, 1918) is a popular method for growing a large size crystal. During the CZ growth, the melt is contained in a crucible, but the crystal is grown at the free top surface of the melt so that there is no contact between the crystal and the crucible. It is the important of the CZ technique that there is less strain in the crystal.

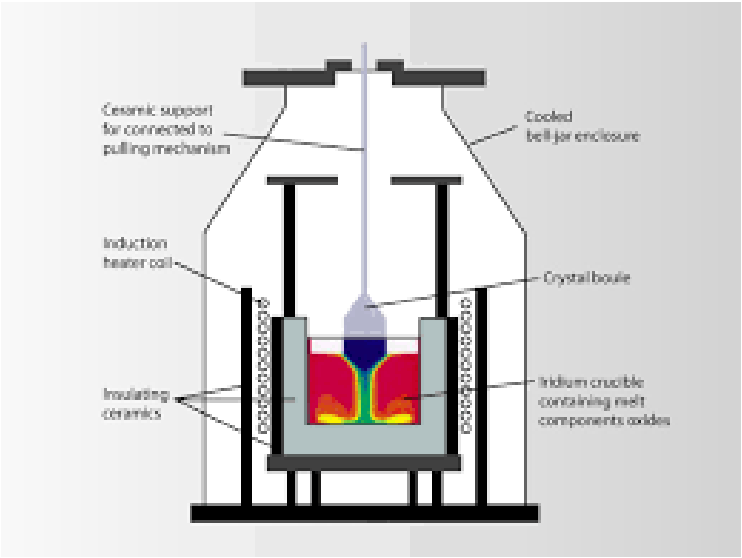

Figure 1. Czochralski Crystal Growth Furnace

The grown crystal is slowly pulled upward as it grows so that the solid-liquid interface is just above the level of the liquid surface. It is observed that crystalline nuclei can develop only if the temperature near crystalline nuclei is lower than melt temperature, that is, the interface between solid and liquid must be in super cooling state. Similarly, the temperature decreases as the crystal grows so that crystallization not only keeps super cooling state at the interface but also transfers heat along that direction. Therefore, the control of the temperature distribution in CZ growth is an essential condition for crystal growth (Brice, et al., 1973 and Zhang, 1981).

Semiconductor materials, especially gallium arsenide (GaAs) single crystal, are very useful in the electronic industry. The single crystal of GaAs provides the material foundation for much of the current semiconductor device technology. It has been applied in the fabrication of short wavelength lasers(< 0.9 J/m), light emitting diodes (LED) and discrete low noise or power field effect transistors (FETs) for microwave use [VonNeida, et al., 1986]. Compared with silicon (Si), GaAs has a high electron mobility. Therefore, it can be used in high speed electronic product. Because of the great application of GaAs substrate for electronic and optoelectronic circuits, it is very important to grow the large size crystal with a low defect. To have a low defect in crystal, the temperature during crystal growth should be controlled. Only a few related research have been carried out on temperature distribution on crystal growth.

Ciszek and Wang (2000). investigated Silicon Float-Zone Crystal Growth As A Tool For The Study Of Defects And Impurities. They observed that The low defect and impurity concentrations obtainable by float zoning allow baseline lifetimes over 20 milliseconds and photovoltaic device efficiencies over 22%, so small effects of impurities and defects can be detected easily.

Knrpnrnrck (1975) studied Crystal Growth from the Melt: A Review. In his review it was discovered that the rate-controlling process may be diffusion in the melt, h eat flow, or the reaction at the crystal-melt interface Diffusion or heat-flow controlled growth generally leads to a cellular morphology. For most silicates, interface-controlled growth leads to a faceted morphology.

Bapuji et al (2008) studied numerically the transient laminar free convection from a vertical cone with non-uniform surface heat flux. They observed The velocity and temperature fields to increases with time. The time taken to reach steady-state increases with increasing Pr or m.. The difference between temporal maximum values and steady state values (for both velocity and temperature) becomes less when Pr or m increases.

Geiser et al (2006) Transient numerical study of temperature gradients during sublimation growth of SiC: Dependence on apparatus design. Using transient and stationary mathematical heat transfer models including heat conduction, radiation, and radio frequency (RF) induction heating, they numerically investigate the time evolution of temperature gradients in axisymmetric growth apparatus during the sublimation growth of silicon carbide (SiC) bulk single crystals by physical vapor transport (PVT) (modified Lely method). They observed that the size of the gradients was found to depend much less on the size of the powder charge, but being slightly smaller for the smaller amount of source powder. The seed temperature established at the end of the heating process and throughout the growth stage did not vary significantly with the considered different designs. The temperature gradients on the seed's growth surface were also found to increase with time and temperature during heating, then to decrease during growth and cooling.

Wang, and Hu (1998) Studied the Concentration distribution in solution crystal growth: effect of moving interface conditions The results show that it is imperative to consider the effect of the moving interfaces on the concentration distribution at the growth interface for some cases.

Jordan (1980) formulated a tractable model for crystal growth, and obtained the temperature distribution in the crystal. This was done by solving the quasi-steady-state partial differential equation for heat conduction subject to appropriate boundary conditions. He considered that the dislocation density is proportional within an additive constant to quantity which is mostly elastic. Furthermore, he set up the critical resolved shear stress (CRSS), which is assumed in most cases to be equal to the lower yield stress obtained by compression testing [Muller, et al., 1985]. Wherever the elastic stresses in the crystal exceed a threshold value (CRSS), dislocations are generated. Since this approach does not provide for differentiation between dislocation nucleation and multiplication, it can not be used for quantitative prediction of dislocation density [Motakef, 1991].

In Czochralski method, the material to be grown is melted by induction or resistance heating under a controlled atmosphere in a suitable non-reacting container. By controlling the furnace temperature, the material is melted. A seed crystal is lowered to touch the molten charge. When the temperature of the seed is maintained very low compared to the temperature of the melt, by suitable water cooling arrangement, the molten charge in contact with the seed will solidify on the seed. Then the seed is pulled with simultaneous rotation of the seed rod and the crucible in order to grow perfect single crystals. Diffusion rates are less and equilibration occurs more slowly at low than at high temperatures. Crystallization may occur more slowly at low than at high temperature. Temperature effects can be more pronounced at low ionic strength reagent conditions.

This present work considers the numerical simulation of the temperature distribution of GaAs Single Crystal using the Czochralski (CZ) Growth Technique.

Mathematical modeling

The temperature distribution of the crucible is solved from the energy equation.

At the high temperatures radiation dominates the energy transport and convection may be neglected. The system changes gradually with time due to the crystal growth. The changes are, however, so slow that the system is assumed to be in a thermally stable state, and the energy equation becomes stationary.

$$-\nabla.(k.\nabla T) = h \qquad 1.$$

Now h is the local heat generation in unit volume which may result from inductive of resistive heating. The energy equation may have fixed (Dirichlet) or flux (Neumann) boundary conditions. Often the flux boundary conditions may be written as

$$-(k.\nabla T).e_n = q(r,T) = h_T\, h(r,T)(T - T_{ext}), \qquad 2.$$

heat transfer by radiation is $q(r,T)=\varepsilon\sigma_{SB}(T^4 - T_{ext}^4)$, 3.

If this is linearized by factorization to the form given by Equation (2) the heat transfer coefficient becomes

$$h_T(r,T) = \varepsilon\sigma_{SB}(T^2 + T_{ext}^2)(\mathrm{T}^4 + \mathrm{T}_{\mathrm{ext}}^4) \quad 4.$$

A special case of radiation is a boundary condition for a surface that sees itself at least partially. This makes the local external temperature dependent on the temperature of the boundary itself. Therefore the external temperature cannot be known *a priori* and must be calculated from the following equation,

$$T_{ext}^4(r) = \frac{1}{\varepsilon(r)} \int \varepsilon(r)G(r^{\rightarrow 1}, r^{\rightarrow 1})T^4(r^{\rightarrow 1})\, ds_{r^{11}} \quad 5.$$

The Gebhart factors are solutions of the integral equation

$$\mathrm{G}(r^{\rightarrow 1}r^{\rightarrow}) - \int F(r^{\rightarrow 1}r^{\rightarrow})(1\text{-}\epsilon(r^{\rightarrow 1}))\ \mathrm{G}(r^{\rightarrow 1}r^{\rightarrow})\ \mathrm{d}s_{r^{11}} = \mathrm{F}(r^{\rightarrow 1}r^{\rightarrow})\epsilon(r^{\rightarrow}) \quad 6.$$

F depends only on geometry of the system

$$\mathrm{F}(\vec{r},\vec{r}) = \frac{cos\beta\,(r^{\rightarrow}r^{\rightarrow 1})cos\beta^{i}(r^{\rightarrow i}r^{\rightarrow 1})}{\pi\left|r^{\rightarrow} - r^{\rightarrow 1}\right|^2}\ \mathrm{x}(r^{\rightarrow}r^{\rightarrow 1}), \quad 7.$$

The boundary conditions must be set on both sides of the gap. For linear heat transfer the boundary condition at the sides are expressed by a dual boundary condition

$$\begin{cases} \mathrm{q}(\vec{\mathrm{r}},T) = h_T(\vec{r},\mathrm{T})(\mathrm{T} - T^i) \\ q^1(\vec{r},T^1) = h_T(\vec{r},\mathrm{T})(T^1 - T) \end{cases}$$

8.

In the case of radiation it is not necessary to calculate the view factors since it is obvious that at the interface the walls see the other side of the gap in a full angle. The heat transfer coefficient may now be analytically calculated to be

$$h_T = \frac{\epsilon\epsilon^1}{\epsilon + \epsilon^1 - \epsilon\epsilon^1}\ \sigma_{SB}\ (\mathrm{T} + T^1)\ (T^2 + T^I) \quad 9.$$

Numerical Models

Numerical solution of the physical models presented in the previous chapter requires some elaborate computational techniques. The outline of the numerical and computational techniques is presented here. The description of equilibrium chemistry leads to a minimization problem with some additional constraints. It could basically be solved with standard methods for

minimization problems. However, low partial pressures may make numerical derivation quite inaccurate.

Therefore general optimization methods may fail and some special methods for the case must be used (Smith and Missen 1982). Most of the physical models are expressed as partial differential equations. The finite element method (FEM) is a standard method for discretization of differential equations in complex geometries (Mohr 1992, Kardestuncer and Norrie 1987, Hämäläinen and Järvinen,1994). It was also the method of choice in this work.

There are different favors of FEM, depending on what kind of elements are used and how the values of functions are calculated inside the elements. In this work, the *standard Galerkin formulation* with linear elements is always used. The advanced features in the FEM calculations deal with the implementation of the specific physical models and the multi-physics features of the code. The finite element method is used to solve the energy equation. This equation will be considered first since the finite element method is most conveniently introduced for this case. The discretization of the differential equation starts with writing the corresponding variational formulation, a so-called *weak form* of the equation. In the axisymmetric case equation (1) yields

$$-\frac{\partial}{\partial z}\left(k_z \frac{\partial T}{\partial Z}\right) - \frac{1}{r}\frac{\partial}{\partial r}\left(k_r\, T \frac{\partial T}{\partial r}\right) = h \qquad 10.$$

where the thermal conductivity tensor is assumed to be diagonal. Integrating over an axisymmetric volume with boundary condition, and applying Green's theorem, Equations (3) and (2) give

$$\int_{\Omega} \left(k_z \frac{\partial v}{\partial z}\frac{\partial T}{\partial z} + k_r \frac{\partial v}{\partial r}\frac{\partial T}{\partial r}\right) \text{r dr dz} + \int_{\Omega} vqrdl = \int_{\Omega} vhrdrdz. \quad \forall v \in \cup \qquad 11.$$

The unknown temperature distribution is expressed as a linear combination of the basis functions φ_i.

$$\text{T}(r^{\rightarrow}) = \sum_{t=1}^{1} t_i \varphi_i(r^{\rightarrow}) \qquad 12.$$

The real-life geometries are seldom rectangular. Therefore also the elements used for discretization should be non rectangular. It is nowadays customary to use *isoparametric elements* to represent the geometry and use local coordinates in assembling the matrix equations. In this work, all the geometries are two-dimensional and only bilinear isoparametric basis functions are used. In the axisymmetric case the global coordinates r and z are expressed with the help of normalized coordinates $\xi \in (-1,1)$ and $\eta \in (-1,1)$

$$\text{r}(\xi,\eta) = \sum_{t=1}^{4} f_i(\xi,\eta) r_{i,}$$

z (ξ,η) = $\sum_1^4 f_i(\xi,\eta)r_i$, 13.

transforms the local point to the global coordinate system. The bilinear isoperimetric element is defined by the following basis functions

$$f_i(\xi,\eta) = \frac{1}{4}(1-\xi)(1-\eta),$$

$$f_2(\xi,\eta) = \frac{1}{4}(1+\xi)(1-\eta),$$

$$f_3(\xi,\eta) = \frac{1}{4}(1+\xi)(1+\eta),$$

$$f_4(\xi,\eta) = \frac{1}{4}(1-\xi)(1+\eta), \quad 14.$$

The basis functions above are local basis functions associated with a given element. They are related to the global basis functions by

$\varphi_i(\vec{r}) = \begin{cases} f_j(\xi,\eta), \\ o, \end{cases}$ if $\vec{r}$ is within an element whose local node j is the global node I 15.

In the Galerkin formulation the basis functions are also used as a set of equation for the unknown temperatures

$\sum_{t=1}^1[\int_\Omega (K_z \frac{\partial\varphi_j}{\partial z}\frac{\partial\varphi_i}{\partial z} + K_r \frac{\partial\varphi_j}{\partial r}\frac{\partial\varphi_i}{\partial r})rdrdz]t_i + \int_{\partial\Omega}\varphi_j q(r^{\rightarrow}t_1,t_2,\dots.,t_N)rdl = \int_\Omega \varphi_j\ hrdrdz, j =$ 1, …,1 16.

The integration is performed numerically using Gaussian quadratures. The procedure results in a matrix equation that may be solved applying standard methods of linear algebra. The type of heat exchange q determines the nature of equation (16). If it is linear with temperature also the total equation is at least pseudo-linear. There might still be temperature dependent parameters, such as the thermal conductivity. If the heat exchange is due to radiation, the equation can still be solved as if it were linear. This requires the use of Equation (4). Linear boundary conditions can be split into two,

$\int_{\partial\Omega}\varphi_j qrdl = \sum_{i=1}^1(\int_\Omega \varphi_j\,\varphi_i\,hrdrdz)t_1 - \int_{\partial\Omega}\varphi_j h_T T_{ext}rdrdz.$ 17.

Here, the first term is linear with respect to T and the second term is constant, or can at least be handled as constant. Truly nonlinear boundary conditions may lead to problems in convergence when treated as linear. This is the case for a boundary that is coupled to itself through the Gebhart factors. The discrete counterpart of Equation (3) is

$q_i = \sigma_{SB} \in_i (T_i^4 - T_{ext}^4)$, 18.

Where

$T_{ext,i}^4 = \frac{1}{A_I \in_I} \sum_{k=1}^{1s} \in_k A_K G_{ki} T_k^4$ 19

. The Gebhart factors *Gji* are solutions of

$G_{ji} - \sum_{k=1}^{I_S} F_{jk} (1 - \epsilon_k) G_{ki} = F_{ji} \epsilon_i$ 20.

$f_{ij} = \frac{1}{A_i} \int_{si} \int_{sj} \frac{cos\beta_i \left(r_i^{\rightarrow} r_j^{\rightarrow}\right) cos\beta_j (r_i^{\rightarrow} r_j^{\rightarrow})}{\pi \left| r_i^{\rightarrow} - r_j^{\rightarrow} \right|^2} \chi(r_i^{\rightarrow}, r_j^{\rightarrow}) \, ds_i ds_j$ 22.

The difference between linear and nonlinear models is important in selecting the best method for solving the equations. Using the linear Iteration the solution satisfies the equation

A(t)t=f(t)

23.

Where

$A_{ji} = \int_{\Omega} (k_z \frac{\partial \varphi_j}{\partial z} \frac{\partial \varphi_i}{\partial z} + k_r \frac{\partial \varphi_j}{\partial r} \frac{\partial \varphi_i}{\partial r}) \, r \, dr \, dz + \int_{\partial \Omega} \varphi_j \varphi_i h_T \, r \, dl$ 24.

And

$\boldsymbol{f_j} = \int_{\Omega} \varphi_j \, hrdrdz, + \int_{\partial \Omega} \varphi_J h_T T_{ext} \, \mathrm{r} \, \mathrm{dl}.$ 25.

The iteration scheme is

$t^{(m+1)} = A^{-1} \left(t^{(m)}\right) \mathrm{f} \, (t^{(m)})$ 26.

Results and discussion

Using the numerical method in the above equations and controlling a few of variables which are time, pull rate, radius, thermal diffusivity, and ambient temperature, we are able to get the temperature distribution. The temperature distribution are in Fig. 2, Fig. 3 and Fig.4 . However, for the rate of pull (p = 0.003 cm/s), the value of the dislocation density is basic less than that in the other two cases at the same location. For the rate of pull is 0.001 cm/s, the value of defect is the highest. We also observe that the defects is basic parallel to radius. And the distance between any two lines is very small. But the values on each are different. In those figures, the growth time is 1 hour, the radius of crystal is 3 cm and the thermal diffusivity is 0.04 cm^2 *I* s. But the rates of pull are different, which are 0.003 cm/s, 0.002 cm/s and 0.001 cm/s, respectively. adjusting the value of the pulling rate, at 0.001 cm/s, 0.002 cm/s as shown in Fig. 2 and Fig. 3, respectively. we saw that the distribution defects occasioned by temperature distribution are similar. To summarize the three cases, we observe that they have similar temperature distributions. The temperature gradient near the edge is greater than that near the center and the temperature gradient decreases as the crystal grows. We recall that the temperature distribution is also strongly varied on the axial location rather

than on the r coordinate. The value for the temperature gradient is extremely large where the axial location is near the melt-solid interface. Therefore, we can say that the high thermal gradient creates the high effective stress.

It can be seen that the temperature distribution at the center point of GaAs melt is more uniform when the process of solidification is finished. The temperature gradient is the driving force for crystal growth and it is desirable to have vertical growth instead of horizontal. Hence, the vertical direction needs to maintain an appropriate temperature gradient and the temperature gradient in a horizontal direction needs to constantly decrease. The temperature of GaAs melt in the central region is higher than that near side boundaries and the heat transports from the central to the side region. The negative temperature gradient is formed and its value increases constantly with the growth of the GaAs. The figures show that as the temperature increases the pull rate increases , the radius of the crystal increases, the temperature distribution is more. It means that the temperature is strongly varied on the axial location (related to <p) rather than r coordinate. The result is consistent with the conclusion we obtained from Jordan's mathematical model.

The first distinguishing characteristic of the temperature distribution is a sharp decrease of temperature near the crystallization front.

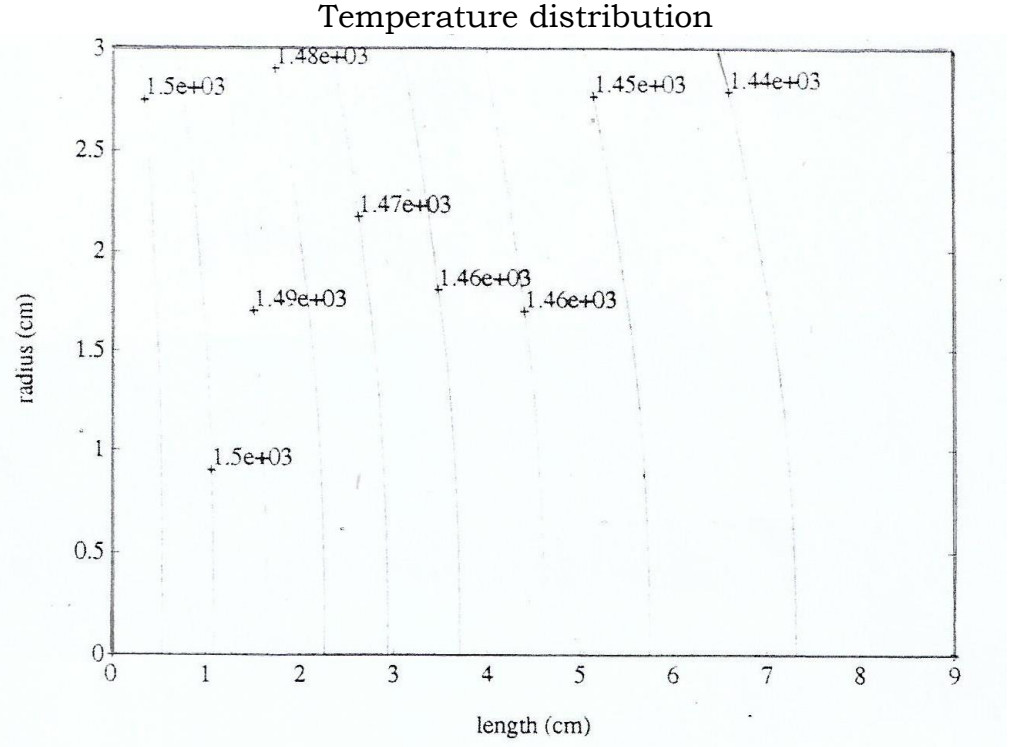

Fig. 2. Temperature distribution of gallium arsenide . the radius of crystal $3x10^{-2}$m, thermal diffusivity $4x\ 10^{-4}m^2/sec$, time of growth 1 hour, pull rate $3x10^{-3}$cm.

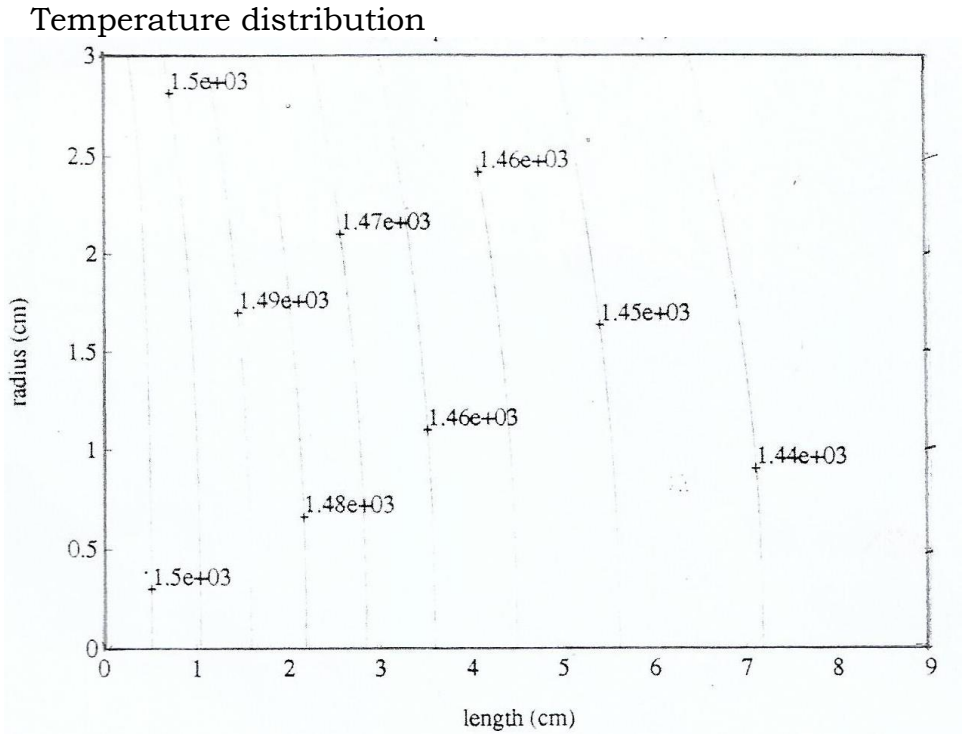

Fig.3. temperature distribution of gallium arsenide , radius of crystal $3x10^{-2}$m, thermal diffusivity $4x\ 10^{-4}m^2$/sec, time of growth 1 hour, pull rate $2x10^{-3}$cm/sec.

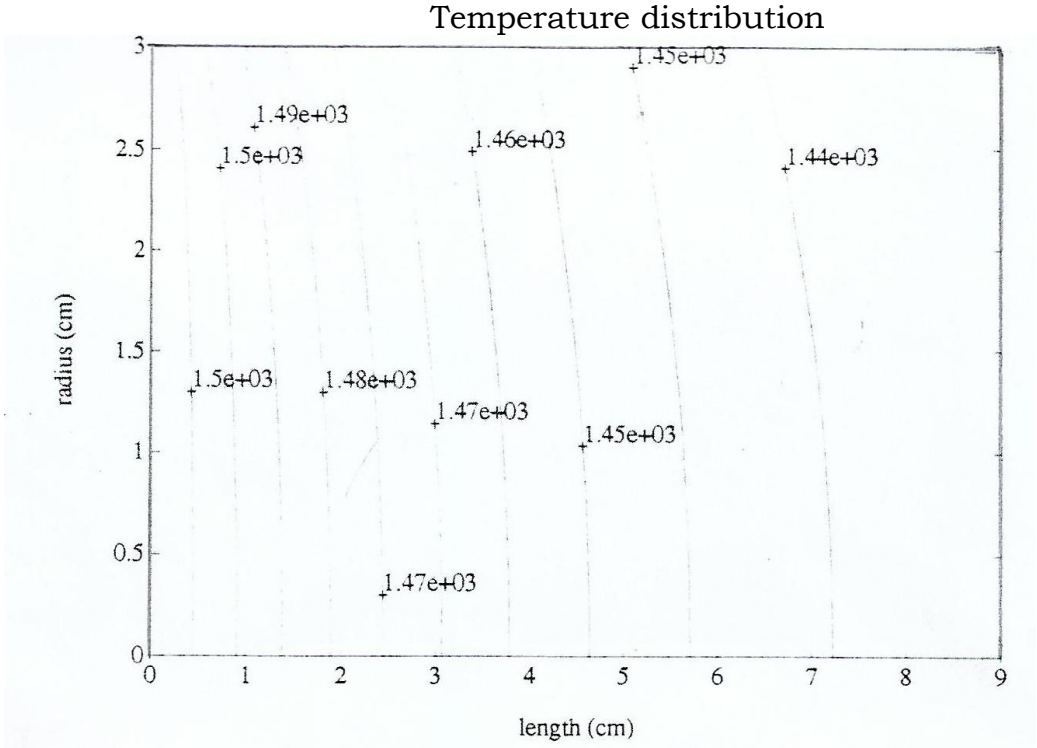

Fig.4. temperature distribution of gallium arsenide , radius of crystal $3x10^{-2}$m, thermal diffusivity $4x10^{-4}m^2$/sec, time of growth 1 hour, pull rate $1x10^{-3}$cm/sec.

Conclusion

We used Jordan's mathematic model [Jordan et al., 1980] to simulate the temperature distribution in the CZ growth of GaAs crystal. The model includes some parameters, such as time, pull rate, axial location, radius, convective and radiative heat transfer coefficients, and a fixed ambient temperature. By controlling those parameters, we can obtain the temperature distribution which will generate a well-distributed dislocation.

References

Bapuji P., Ekambavanan, J., & Pop, I. (2008). Transient Laminar Free Convection From A Vertical Cone With Non-Uniform Surface Heat Flux, *Studia Univ. "Babes¸–Bolyai", Mathematica, 53, (1), 12 – 19.*

Brice, J. C.,(1973). "Analysis of the temperature distribution in pulled crystals," *Journal of. Crystal. Growth, (2) 395- 405.*

Ciszek, T.F. & Wang, T. H. (2000). investigated Silicon Float-Zone Crystal Growth As A Tool For The Study Of Defects And Impurities. *presented at the Electrochemical Society Fall Conference Phoenix, Arizona October 22-27.*

Czochralski, T., Z. Physics of semi conductor. 1918.

Hämäläinen, J. & Järvinen, J. (1994). *Elementtimenetelmä virtauslaskennassa*. CSC _ Tieteellinen laskenta Oy,

Hyun, Y., Roland, L., & Theophilus, O. (2008). The Growth of Ice Crystals by Molecular Diffusion, *Journal Of The Atmospheric Sciences. 63, 123-128.*

Jordan, A. S., (1980)."An evaluation of the thermal and elastic constants affecting GaAs crystal growth," *Journal of Crystal Growth, 49, 631-638.*

Jurgen G., Olaf, K, & Peter P. (2006). Transient numerical study of temperature gradients during sublimation growth of SiC: Dependence on apparatus design. *Journal of Crystal Growth 297, 20–32*

Kardestuncer, H. & Norrie, D. H. (1987). *Finite Element Handbook*. McGraw-Hill Book Company.

Kitanin, E. L., Ramm, M. S., Ris, . V. V & Schmidt. A. A. (1998). Heat transfer through source powder in sublimation growth of SiC crystal. *Materials Science and Engineering, 174-183.*

Knrpnrnrcr, R.J.(1975). Crystal Growth from the Melt: A Review. *American M ine ralogist, (60) 798-614.*

Mohr. G. A. (1992). Finite Elements for Solids, Fluids, and Optimization. Oxford University Press

Müller, St. G., Ecktsein, . R., Fricke, J., Hofmann, D., Hofmann, R., Horn, R., Mehling, H. & Nilsson. O. (1998). Experimental and theoretical analysis of the high temperature thermal conductivity of monocrystalline SiC. *Materials Science Forum*, 264-268.

Motakef, S., (1991)."A high temperature creep model for GaAs," *Journal of Crystal Growth, 108, 36-47.*

Pardeep K. & Mohan, H. (*2012).* Double-Diffusive Convection in Compressible Viscoelastic Dusty Fluid Through Brinkman Porous Media. *American Journal of Fluid Dynamics , 2(2): 1- 6.*

Smith W. R. & Missen. R. W (1982). *Chemical Reaction Equilibrium Analysis: Theory and Algorithms*. Krieger Publishing Company.

VonNeida, A. R., Timoshenko, S. P. & Goodier, J. N., "On the prediction of dislocation formation in semiconductor crystals grown from the melt. *Journal of Metals, June, 1986.*

Wang, W.. Hu, W.R (1999). Concentration distribution in solution crystal growth: effect of moving interface conditions. *Journal of Crystal Growth 203 . 227-233.*

Zhang, K. C., (1989.). Yield points and delay times in single, *Journal of Crystal Growth, 165, 176 – 184.*